Available online at www.sciencedirect.com
SCIENCE DIRECT®
Journal of Catalysis 222 (2004) 143–151
JOURNAL OF CATALYSIS
www.elsevier.com/locate/jcat

Evaluation of the maximum potential activity of Co–Mo/Al_2O_3 catalysts for hydrodesulfurization

Yasuaki Okamoto,* Keiji Ochiai, Masatoshi Kawano, and Takeshi Kubota

Department of Material Science, Shimane University, Matsue 690-8504, Japan

Received 10 July 2003; revised 6 October 2003; accepted 21 October 2003

Abstract

Co *K*-edge XANES results confirmed the previous findings that a selective formation of Co atoms in a CoMoS phase is achieved by means of a CVD technique using $Co(CO)_3NO$. If MoS_2/Al_2O_3 is exposed to $Co(CO)_3NO$ vapor and subsequently sulfided, the resultant catalyst exhibits the maximum potential activity of Co–Mo/Al_2O_3 catalysts based on the MoS_2/Al_2O_3. This activity is obtained when the edges of the MoS_2 particles are fully occupied by Co atoms without any blocking by Co sulfide clusters. With Co–MoS_2/Al_2O_3 catalysts prepared by classic impregnation, the edge sites of MoS_2 particles remain unoccupied by Co atoms in a wide range of Co content. In contrast, the edges of MoS_2 particles are completely occupied by Ni atoms above 2 wt% Ni. Blocking of the active sites by overlayers of Co(Ni) sulfide clusters decreases the HDS activity to a considerable extent. The CVD technique with $Co(CO)_3NO$ as the probe molecule provides a novel characterization method for Co(Ni)–Mo sulfide catalysts, giving information about (i) the maximum potential HDS activity, (ii) the extent of blocking of the active phase, (iii) the coverage of Co(Ni) atoms on the edges of the MoS_2 particles, and (iv) the dispersion of MoS_2 particles in Co(Ni)–MoS_2 catalysts.

Keywords: Co–Mo catalysts; Ni–Mo catalysts; HDS; Surface structure; Co carbonyl; Co *K*-edge XANES

1. Introduction

The development of highly active ultradeep hydrodesulfurization (HDS) catalysts has been one of the most urgent issues in the petroleum industry to meet the increasing demand to further reduce sulfur contents in fuels to 15 ppm (USA, 2006) and then to less than 10 ppm (sulfur free) in the near future [1,2]. Supported Mo sulfides promoted by Co or Ni are still the main active components of ultradeep HDS catalysts [3–6]. Additions of a chelating agent [7–11] and phosphorus [12–16] have been reported to be very effective in improving the activity of Co(Ni)–Mo catalysts. The catalytically active phase in promoted catalysts has been proposed by Topsøe and coworkers [4,17–19] to be a Co(Ni)MoS phase, where Co(Ni) atoms are located on the edges of the MoS_2 particles. They found that there are two types of CoMoS phases with distinctly different HDS activities, CoMoS type I and type II, the latter exhibiting about two times higher activity than the former [20]. It is, accordingly, expected that highly active HDS catalysts are composed of a highly dispersed CoMoS type II phase. It is also very effective in increasing the coverage of Co on the edges of MoS_2 particles. For this purpose, chelating agents play an important role by forming complexes with increased thermal stability [11,21–25].

During the development of HDS catalysts, it would be very informative to gain knowledge on how far the activity of a catalyst under study can be improved by increasing the coverage of Co on the edges of the MoS_2 particles. In a previous study [26], we suggested, for the first time, a method to evaluate the maximum potential HDS activity of Co–Mo/Al_2O_3 catalysts by the use of $Co(CO)_3NO$. In the present study, we systematically extend the evaluation method to Co–Mo/Al_2O_3 and Ni–Mo/Al_2O_3 catalyst systems. Furthermore, we propose a novel characterization method of the surface structure of Co(Ni)–Mo/Al_2O_3 catalysts by using $Co(CO)_3NO$ as a probe molecule.

* Corresponding author.
E-mail address: yokamoto@ifse1.riko.shimane-u.ac.jp (Y. Okamoto).

0021-9517/$ – see front matter
doi:10.1016/j.jcat.2003.10.024

2. Experimental

2.1. Catalyst preparation

A MoO_3/Al_2O_3 catalyst with 8.7 wt% Mo was prepared by an impregnation technique using $(NH_4)_6Mo_7O_{24}\cdot 4H_2O$ (Kanto Chemicals, analytical grade). After evaporation of the impregnation solution to dryness at ca. 350 K while stirring, the catalyst was dried at 383 K for 16 h. The catalyst was calcined in air at 773 K for 5 h. Al_2O_3 (JRC-ALO-7: 180 m^2/g) was supplied by the Catalysis Society of Japan as a Reference Catalyst. Aliquots of MoO_3/Al_2O_3 were used to prepare CoO–MoO_3/Al_2O_3 and NiO–MoO_3/Al_2O_3 catalysts having various Co or Ni contents.

A series of CoO–MoO_3/Al_2O_3 catalysts (Co content: 0.5–10 wt%) was prepared by impregnating MoO_3/Al_2O_3 with an aqueous solution of $Co(NO_3)_2$ (double impregnation, an incipient wetness method). After the impregnation, the catalysts were dried at 383 K for 16 h and subsequently calcined at 773 K for 5 h. A series of NiO–MoO_3/Al_2O_3 catalysts (Ni content: 0.5–10 wt%) was also prepared in a similar way using $Ni(NO_3)_2$ as a precursor.

The MoO_3/Al_2O_3 and CoO(NiO)–MoO_3/Al_2O_3 catalysts were sulfided at 673 K in a 10% H_2S/H_2 flow [26,27]. The Mo sulfide catalyst is designated MoS_2/Al_2O_3. The Co(Ni)–Mo sulfide catalyst is simply denoted Co(Ni)–MoS_2/Al_2O_3. The Co or Ni content is given when necessary.

MoS_2/Al_2O_3 or Co(Ni)–MoS_2/Al_2O_3 was evacuated at 673 K for 1 h prior to exposure to a vapor of $Co(CO)_3NO$ at room temperature (CVD technique) [26,27]. After evacuation at room temperature, the sample was sulfided again at 673 K to produce a Co–Mo sulfide catalyst. The catalyst prepared using $Co(CO)_3NO$ is denoted CVD-Co/MoS_2/Al_2O_3 when MoS_2/Al_2O_3 was used or CVD-Co/Co(Ni)–MoS_2/Al_2O_3 when Co(Ni)–MoS_2/Al_2O_3 (Co or Ni content, 0.5–10 wt%) was modified.

The amount of Co anchored by the CVD technique was determined for the sulfided catalyst by means of XRF (Rigaku RIX 2000) with an accuracy of 0.05 wt% Co. The catalyst sample (ca. 0.1 g) was mixed well with HY zeolite powder (ca. 0.6 g) and $Li_2B_4O_7\cdot 5H_2O$ (3.5 g) to make a glass bead for the XRF measurements. A linear calibration curve was obtained by using CoO/Al_2O_3 (1–10 wt% Co).

2.2. Reaction procedure

The activity of the freshly prepared catalyst for the HDS of thiophene was evaluated at 623 K and an initial H_2 pressure of 20 kPa using a circulation system made of glass. The thiophene pressure was kept constant (2.6 kPa) during the reaction [26,27]. The products were mainly C_4 compounds and a corresponding amount of H_2S. The HDS activity was calculated on the basis of the accumulated amount of H_2S.

2.3. Characterization

The amount of NO adsorption on MoS_2/Al_2O_3 was measured at room temperature by a pulse technique [26–28] after cooling from 673 K in a H_2S/H_2 stream. The sample was purged with a high-purity He stream before periodic introduction of NO pulses. The amount of NO adsorption was not significantly changed by evacuation at 673 K for 1 h prior to the adsorption. The reproducibility was usually better than ±5% of the total amount of NO adsorption.

Co *K*-edge XANES spectra for CVD-Co/MoS_2/Al_2O_3, CVD-Co/Al_2O_3, Co–MoS_2/Al_2O_3, and reference compounds were measured in the fluorescence mode at room temperature using an in situ XAFS cell with Kapton windows. The spectra were recorded at BL-7C in the Photon Factory of Institute of Materials Structure Science, High Energy Accelerator Research Organization (KEK-IMSS-PF), with 2.5 GeV ring energy and 250–290 mA stored current by using a Lytle-type detector. The higher harmonics were eliminated by detuning the incident X-ray intensity to 60%. The scan step was 0.5 eV. The synchrotron radiation was monochromatized by a Si(111) double-crystal monochromator. Normalized XANES spectra were obtained by subtracting the preedge background from the raw data assuming a straight line. Normalization was carried out by the edge height.

3. Results

3.1. Co K-edge XANES spectra

Fig. 1 presents the Co *K*-edge XANES spectra of CVD-Co/MoS_2/Al_2O_3, CVD-Co/Al_2O_3, and Co–MoS_2/Al_2O_3 having 1, 2, and 4 wt% Co. The spectra for Co_9S_8 and "$CoAl_2O_4$" (Co^{2+} in Al_2O_3 subsurface), which was prepared by calcination of 3 wt% CoO/Al_2O_3 at 973 K for 5 h, are also shown for comparison. The XANES spectrum of CVD-Co/Al_2O_3 showed spectral features common to those of Co_9S_8: a broad band around 7725 eV and a peak at 7715 eV. However, the 1s-3d preedge peak at 7707 eV and the peak at 7715 eV were considerably weaker in intensity than those for Co_9S_8. A comparison of the difference spectra (Fig. 2a) of CVD-Co/Al_2O_3 and Co_9S_8 from that of CVD-Co/MoS_2/Al_2O_3 highlights the similarities and dissimilarities between these spectra in Fig. 1. Fig. 2a suggests that the electronic and local structures of Co sulfide clusters in CVD-Co/Al_2O_3 are different from those in Co_9S_8. In contrast, Fig. 1 shows that the broad structures around 7725 eV, characteristics of Co sulfide clusters, is absent in the spectrum of CVD-Co/MoS_2/Al_2O_3. This is clearly illustrated in the difference spectrum in Fig. 2a ([CVD-Co/Al_2O_3] − [CVD-Co/MoS_2/Al_2O_3]) and indicates an extensive change in the local structure of Co in the presence of MoS_2. Furthermore, the intensity of the preedge peak of CVD-Co/MoS_2/Al_2O_3 is even weaker than that of CVD-Co/Al_2O_3, suggesting a

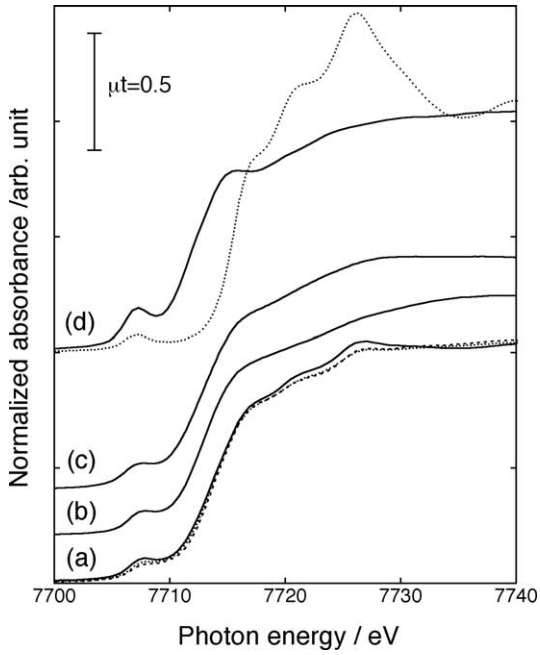

Fig. 1. Co K-edge XANES spectra of (a) Co–MoS_2/Al_2O_3 (dashed line, 1 wt% Co; dotted line, 2 wt% Co; and solid line, 4 wt% Co), (b) CVD-Co/MoS_2/Al_2O_3, (c) CVD-Co/Al_2O_3, and (d) Co_9S_8 (solid line) and "$CoAl_2O_4$" (dotted line).

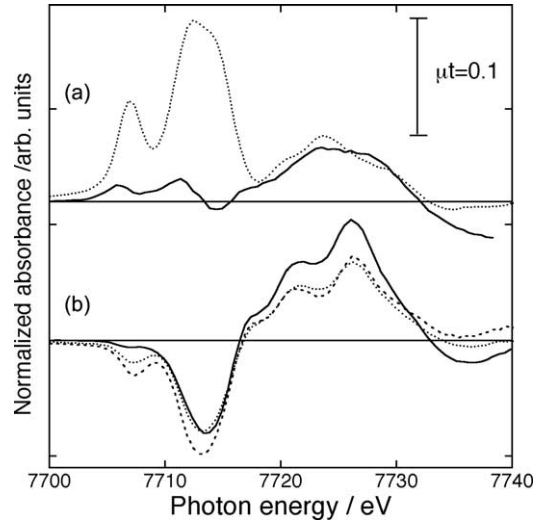

Fig. 2. Difference spectra of Co K-edge XANES of (a) CVD-Co/Al_2O_3 (solid line) and Co_9S_8 (dotted line) and of (b) 1 wt% Co–MoS_2/Al_2O_3 (dashed line), 2 wt% Co–MoS_2/Al_2O_3 (dotted line), and 4 wt% Co–MoS_2/Al_2O_3 (solid line). The XANES spectrum of CVD-Co/MoS_2/Al_2O_3 was subtracted from each spectrum.

further increase in the local symmetry around the Co atoms in the presence of MoS_2.

With the impregnation catalysts, two additional peaks are present around 7721 and 7726 eV. The difference spectra for these catalysts in Fig. 2b ([Co–MoS_2/Al_2O_3] − [CVD-Co/MoS_2/Al_2O_3]) are very close to the spectral features for _$CoAl_2O_4$_ in Fig. 1. The intensity is similar for 1 and 2 wt% Co and is larger at 4 wt% Co. Figs. 1 and 2b demonstrate that Co^{2+} cations remain in the Al_2O_3 subsurface layer after the sulfidation, in agreement with other studies [29]. The negative peak around 7707 eV in Fig. 2b is a contribution of the 1s-3d preedge peak. The intensity of the negative peak decreased as the Co content increased with a concomitant slight shift of the peak position to lower energy (0.5 eV). These changes suggest that the fraction of Co sulfide clusters increases, in particular, at 4 wt% Co. This is consistent with the Co distribution obtained by means of Mössbauer emission spectroscopy for sulfided Co–Mo catalysts having various Co contents [29].

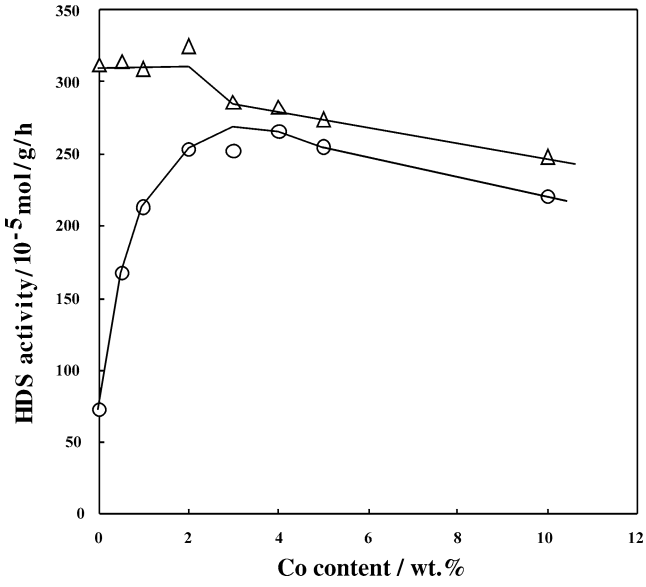

Fig. 3. Catalytic activity of Co–MoS_2/Al_2O_3 (circle) and CVD-Co/Co–MoS_2/Al_2O_3 (triangle) for the HDS of thiophene as a function of Co content in Co–MoS_2/Al_2O_3.

3.2. HDS activity of CVD-Co/Co–MoS_2/Al_2O_3

The HDS activity of Co–MoS_2/Al_2O_3 is shown in Fig. 3 as a function of the Co content. A maximum activity was attained around 3 wt% Co or Co/Mo = 0.56 in agreement with general observations [4]. The activity of Co–MoS_2/Al_2O_3 was significantly promoted by the addition of Co by using $Co(CO)_3NO$ over the whole range of Co content. It is worth noting that if the Co content is lower than 2 wt%, the CVD-Co/Co–Mo/Al_2O_3 catalysts show an identical activity as the CVD-Co/MoS_2/Al_2O_3 catalyst, whereas the activity of the CVD-Co/Co–MoS_2/Al_2O_3 catalysts gradually decreases with increasing Co content at above 2 wt%.

The Co content of the CVD-Co/Co–MoS_2/Al_2O_3 catalysts and the increase in the Co content by the CVD method (difference between the Co contents of CVD-Co/Co–MoS_2/Al_2O_3 and Co–MoS_2/Al_2O_3) are shown in Fig. 4 as a function of the Co content in Co–MoS_2/Al_2O_3. It is obvious that virtually the same amount of Co is anchored by using $Co(CO)_3NO$ irrespective of the original Co content in Co–MoS_2/Al_2O_3 except for the catalysts with more than

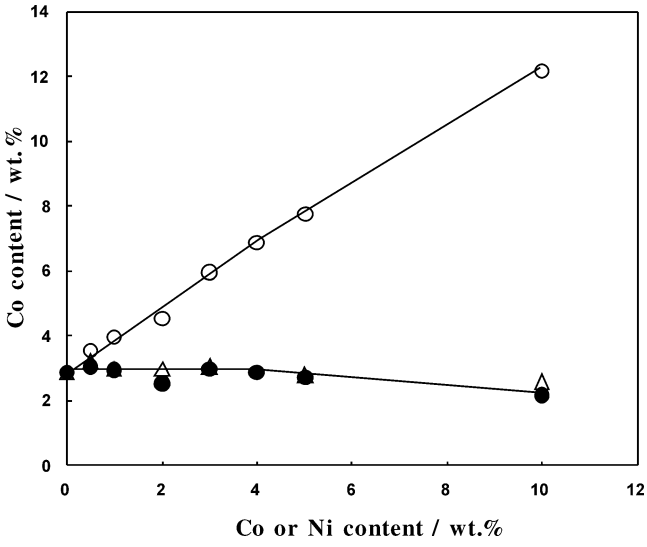

Fig. 4. Amounts of Co in CVD-Co/Co–MoS_2/Al_2O_3 and CVD-Co/Ni–MoS_2/Al_2O_3 as a function of Co or Ni content in the original catalyst. Circle, total amount of Co in CVD-Co/Co–MoS_2/Al_2O_3; (closed circle) Incremental amount of Co in CVD-Co/Co–MoS_2/Al_2O_3 and (triangle) amount of Co in CVD-Co/Ni–MoS_2/Al_2O_3.

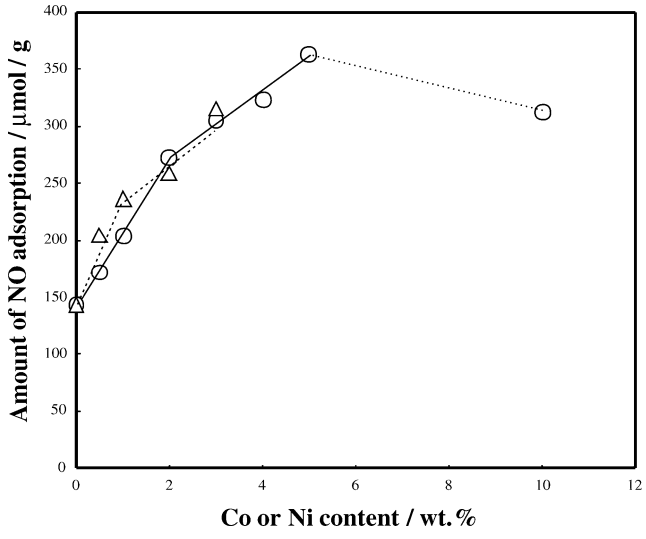

Fig. 5. Amounts of NO adsorption on (circle) Co–MoS_2/Al_2O_3 and (triangle) Ni–MoS_2/Al_2O_3 as a function of Co content in Co–MoS_2/Al_2O_3 or Ni content in Ni–MoS_2/Al_2O_3.

4 wt% Co, which anchor a slightly decreasing amount of Co with increasing Co content.

The amount of NO adsorption on Co–MoS_2/Al_2O_3 was measured to gain some insights into the origin of the activity decrease observed above 2 wt% Co in Fig. 3. The amount of NO adsorbed on Co–MoS_2/Al_2O_3 is shown in Fig. 5 as a function of the Co content. The NO adsorption capacity linearly increased as the Co content increased to 2 wt% Co. Above 2 wt% Co, it increased further but with a smaller increase rate. The amount of NO adsorption decreased above 6 wt% Co.

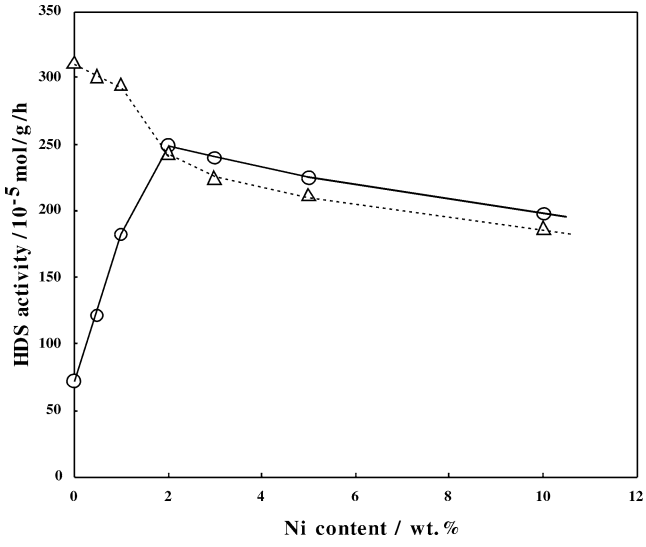

Fig. 6. Catalytic activity of Ni–MoS_2/Al_2O_3 (circle) and CVD-Co/Ni–MoS_2/Al_2O_3 (triangle) for the HDS of thiophene as a function of Ni content in Ni–MoS_2/Al_2O_3.

3.3. HDS activity of CVD-Co/Ni–MoS_2/Al_2O_3

Fig. 6 shows the HDS activity of Ni–MoS_2/Al_2O_3 as a function of Ni content. A maximum HDS activity was attained around 2 wt% Ni. Evacuated Ni–MoS_2/Al_2O_3 was exposed to a vapor of $Co(CO)_3NO$, followed by evacuation and subsequent resulfidation at 673 K to form CVD-Co/Ni–MoS_2/Al_2O_3. As shown in Fig. 6, the HDS activity of Ni–MoS_2/Al_2O_3 was greatly increased by the addition of Co, when the Ni content was lower than 1 wt%. The activity of CVD-Co/Ni–MoS_2/Al_2O_3 slightly decreased as the Ni content increased up to 1 wt%. In contrast, the activity of CVD-Co/Ni–MoS_2/Al_2O_3 decreased considerably above 1 wt% Ni and was slightly lower than that of Ni–MoS_2/Al_2O_3 above 2 wt%. Fig. 4 shows the amount of Co anchored on Ni–MoS_2/Al_2O_3 as a function of Ni content in the Ni–MoS_2/Al_2O_3 catalysts. It is important to note that the amount of Co in the CVD-Co/Ni–MoS_2/Al_2O_3 catalysts is identical with the incremental amount of Co in the CVD-Co/Co–MoS_2/Al_2O_3 catalysts.

Fig. 5 presents the amounts of NO adsorption on the Ni–MoS_2/Al_2O_3 catalysts as a function of Ni content. The amount of NO adsorption increased linearly as the Ni content increased below 1 wt% Ni, followed by a smaller increase above 1 wt% Ni.

4. Discussion

4.1. Selective preparation of a CoMoS phase

First, we will discuss the chemical state of the Co atoms anchored on MoS_2/Al_2O_3 by means of the CVD technique using $Co(CO)_3NO$. The previous XPS results [27] showed that the Co $2p_{3/2}$ binding energy for CVD-Co/MoS_2/Al_2O_3

was 0.8 eV higher (when referenced to the Al 2p level) than that for CVD-Co/Al_2O_3, evidently demonstrating, within the accuracy of the resolution of XPS, the selective formation of Co sulfide species interacting with Mo sulfides. In agreement with the XPS results, the Co *K*-edge XANES of CVD-Co/MoS_2/Al_2O_3 is slightly but significantly different from that of CVD-Co/Al_2O_3 as illustrated in Figs. 1 and 2a. The intensity of the 1s-3d prepeak for CVD-Co/MoS_2/Al_2O_3 is considerably smaller than that for Co_9S_8, in which Co atoms are mainly in a tetrahedral symmetry, indicating that Co species in CVD-Co/MoS_2/Al_2O_3 are in octahedral or square-pyramidal configurations. This is consistent with the XANES observations for a Co(Ni)MoS phase [10,30–32]. The finding that the preedge peak intensity of CVD-Co/Al_2O_3 is intermediate between those of Co_9S_8 and CVD-Co/MoS_2/Al_2O_3 suggests that part of Co sulfide species are in octahedral or square-pyramidal configurations. Crajé et al. [31] showed by XAFS combined with Mössbauer emission spectroscopy (MES) that the Co atoms in carbon-supported ultra-dispersed Co sulfide particles are in an octahedral symmetry. It is, therefore, concluded that the formation of Co atoms in the high symmetry in CVD-Co/Al_2O_3 is caused by a small size of highly dispersed Co sulfide clusters and/or by specific interactions of Co atoms with the Al_2O_3 surface.

On the basis of the proportional relation between the Co/Mo atomic ratio for CVD-Co/MoS_2/Al_2O_3 and the NO/Mo molar ratio for MoS_2/Al_2O_3, it has been suggested [26,27] that the Co atoms are located on the edges of MoS_2 particles, since it is well established [4] that NO molecules adsorb on edge sites rather than on basal planes. The FT-IR spectra of NO adsorption on CVD-Co/MoS_2/Al_2O_3 indicated that the NO adsorption sites of MoS_2/Al_2O_3 are practically completely occupied by Co atoms by a single CVD procedure, showing that Co atoms cover the NO adsorption sites of MoS_2, that is, the edges of MoS_2 particles [33]. With conventional Co–Mo catalysts, Topsøe and Topsøe [18] demonstrated by means of FT-IR that NO molecules adsorbed on the edges of MoS_2 are gradually replaced by those on Co sites with increasing Co content. Furthermore, the activity of CVD-Co/MoS_2/Al_2O_3 was almost invariant or even slightly lower when dosing a second portion of $Co(CO)_3NO$, although the Co content was almost doubled [33]. Summarizing these results, it is concluded that the CVD technique selectively produces Co sulfide species interacting with the edges of the MoS_2 particles, in agreement with the XANES spectra. The preferential interaction of $Co(CO)_3NO$ with supported MoS_2 particles was also suggested by Maugé et al. [34] by means of the FT-IR of CO adsorption. Maugé et al. [34] also demonstrated that the HDS activity of the ex-carbonyl catalysts is linearly correlated to the amount of Co. Recently, we showed [27] that the activity for the HDS of thiophene is proportional to the amount of Co anchored on MoS_2 particles supported on TiO_2, ZrO_2, and Al_2O_3. These properties of Co sulfide species are characteristic of the CoMoS phase proposed by Topsøe and co-workers [4,17–19]. The XANES, XPS [27], FT-IR of NO adsorption [33], and the effect of the CVD cycle on the catalytic activity [33] confirm that a CoMoS phase is selectively and fully formed on the edges of MoS_2 particles supported on Al_2O_3 by means of the present CVD technique. In our previous study [26], it was shown that a selective formation of a CoMoS phase is limited to a supported Mo catalyst in which the Mo content corresponds to or exceeds the monolayer loading on the support.

4.2. Evaluation of the maximum potential HDS activity of Co–Mo sulfide catalysts

It was established by Topsøe and co-workers [4,17–19] that the HDS activity of Co–Mo catalysts is proportional to the amount of Co atoms forming a CoMoS phase. It is, therefore, logic to propose that the highest activity is obtained when all the edge sites of MoS_2 particles are occupied by Co atoms forming a CoMoS phase, that is, when the amount of a CoMoS phase is maximized. As a consequence, when a Mo/Al_2O_3 catalyst is subjected to promotion by Co by means of, for instance, impregnation techniques, the maximum HDS activity attainable is the activity of a CVD-Co/MoS_2/Al_2O_3 catalysts, since the Co atoms are selectively and fully located on the edges of MoS_2 particles in the CVD-Co/MoS_2/Al_2O_3 catalyst.

Fig. 3 shows that the HDS activity of Co–MoS_2/Al_2O_3 is increased by the addition of Co to a different extent, depending on the Co content in the original catalyst. First, we will discuss the activity increase of Co–MoS_2/Al_2O_3 with a low Co content (< 2 wt% Co). In this region of Co loading, the activity of the CVD-Co/Co–MoS_2/Al_2O_3 catalysts is independent of the Co content and identical with that of CVD-Co/MoS_2/Al_2O_3. These results are explained simply in terms of the increase in the coverage of Co atoms on the edges of the MoS_2 particles by the addition of Co by means of the CVD technique. The extent of activity increase reflects the edge coverage of Co atoms in the original Co–MoS_2/Al_2O_3 catalyst. In addition, the constant activity of the CVD-Co/Co–MoS_2/Al_2O_3 catalysts indicates that the dispersion and stacking number of the MoS_2 particles are not significantly modified by the double impregnation process and subsequent sulfidation procedure. This is substantiated by the constant amount of Co anchored by the CVD technique in Fig. 4 (vide infra). Hence, it is concluded that below 2 wt% Co, the potential activity of Co–MoS_2/Al_2O_3 catalysts is not fully generated because of a too low content of the CoMoS phase. The HDS activity of CVD-Co/MoS_2/Al_2O_3, in which the amount of a CoMoS phase is maximized, therefore, shows the maximum potential activity of Co–MoS_2/Al_2O_3.

As discussed above, the XPS [27], XANES, FT-IR of NO adsorption [33], and CVD cycle [33] show that the amount of Co anchored on MoS_2/Al_2O_3 is the amount of the CoMoS phase. As shown in Fig. 4, the same amount of additional Co is incorporated into Co–MoS_2/Al_2O_3 by means of the CVD

technique below 4 wt% Co. The amount of anchored Co is proportional to the dispersion of the MoS_2 particles [26,27]. Assuming that irrespective of the presence of promoter Co atoms, $Co(CO)_3NO$ molecules chemisorb on the edge sites of MoS_2 particles, it is suggested that the dispersion of the MoS_2 particles is not modified by the presence of Co. As suggested previously [26], the adsorbed $Co(CO)_3NO$ molecules are transformed to a CoMoS phase, if the edge sites are vacant for Co accommodation. $Co(CO)_3NO$ molecules adsorbed on the edge sites of MoS_2 particles already occupied by promoter Co(Ni) atoms are converted to less active, separate Co sulfide clusters, which do not form overlayers on the CoMoS phase to a significant extent.

4.3. Blocking of active sites by Co sulfide clusters

When the Co content in Co–MoS_2/Al_2O_3 is higher than 2 wt%, the HDS activity of CVD-Co/Co–MoS_2/Al_2O_3 decreases parallel to the activity of Co–MoS_2/Al_2O_3, as shown in Fig. 3. The increase rate of the amount of NO adsorption becomes smaller at a Co content higher than 2 wt% (Fig. 5). These results can be explained by an increasing extent of blocking of the MoS_2 edges and the CoMoS phase by overlayers of coexisting Co sulfide clusters with increasing Co content above 2 wt% Co. The existence of Co sulfide clusters is suggested by the difference XANES spectrum in Fig. 2b for 4 wt% Co–MoS_2/Al_2O_3. This is also consistent with MES results for Co–Mo/Al_2O_3 catalysts [29]. A surface model of Co–MoS_2/Al_2O_3 is schematically presented in Fig. 7 for clarity. The present model does not exclude the possible formation of separate Co sulfide clusters. As illustrated in Fig. 7, the increase in the activity of Co–MoS_2/Al_2O_3 by the addition of $Co(CO)_3NO$ is ascribed to the increase in the amount of a CoMoS phase. Even at a high Co content, vacant sites for a CoMoS phase remain on the edges of MoS_2 particles in Co–MoS_2/Al_2O_3. This is in agreement with the FT-IR spectra of NO adsorption on sulfided Co–Mo/Al_2O_3 impregnation catalysts reported by Topsøe and Topsøe [18]. Their spectra showed the doublet bands due to NO adsorbed on Mo sites at a high Co content.

Based on the MES and XAFS studies of supported Co–Mo catalysts, Crajé et al. [31,35,36] and van der Kraan et al. [37] proposed a sophisticated surface model of the catalysts, in which highly dispersed Co sulfide particles are located at the edge positions of MoS_2 crystallites and the size of the Co sulfide particles decreases as the Co/Mo ratio decreases. The blocking of the edges of MoS_2 particles by Co sulfide clusters can be easily explained by their surface model. In addition, the fact that the extent of the blocking increases with increasing Co content may be a consequence of the increasing size and number of Co sulfide clusters. It is considered from Fig. 3 that below 2 wt% Co, the size of the Co sulfide clusters becomes ultimately small to form Co sulfide dimer clusters [28,38] on the edges of MoS_2 particles. It is estimated that the consumption of the Co atoms in the CoMoS phase by Co sulfide clusters in contact with them and/or lower reactivity of enlarged and stabilized Co clusters toward the edges of MoS_2 particles results in the decrease in the amount of the CoMoS phase at a high Co content, giving the maximum amount of a CoMoS phase, as observed by means of MES for a series of Co–Mo/Al_2O_3 catalysts with varying Co contents [29]. Nevertheless, we cannot rule out the possibility of a slight decrease in the dispersion of the MoS_2 particles in the presence of Co for the decreases in the HDS activity (Fig. 3) and the amount of anchored Co (Fig. 4).

The maximum activity of Co–MoS_2/Al_2O_3, observed at about 3 wt% Co, is lower than the activity of CVD-Co/MoS_2/Al_2O_3, the maximum potential HDS activity. This is explained in terms of the formation of overlayers and resultant blocking of the active sites by almost inactive Co sulfide clusters before the edge sites of MoS_2 particles are fully occupied by Co atoms. Accordingly, the difference between the activities of CVD-Co/MoS_2/Al_2O_3 and CVD-Co/Co–MoS_2/Al_2O_3 shows the extent of blocking of the active sites, which increases as the Co content increases, as expected.

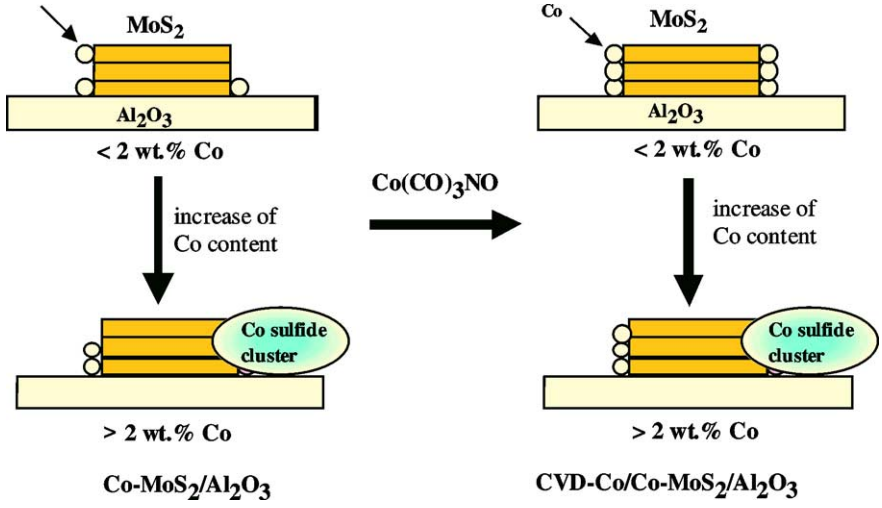

Fig. 7. Schematic surface models of Co–MoS_2/Al_2O_3 and CVD-Co/Co–MoS_2/Al_2O_3.

The activity difference would depend on the catalyst preparation and support through the changes in the distribution, dispersion, chemical state, and sulfidation temperature of the Co atoms. It is well established [11,21–25] that the use of chelating agents increases the sulfidation temperature of Co by the formation of thermally stabilized complexes, facilitating a selective location of Co atoms on the edge sites of preformed MoS_2 particles and thus decreasing the fraction of separate Co sulfide clusters, part of which may block the active sites of the catalyst. In this sense, the effects of the addition of chelating agents in catalyst preparations are twofold.

In our previous study [26], the effect of calcination of Co–Mo/Al_2O_3 (9.1 wt% Mo and 2.7 wt% Co, double impregnation) was briefly studied by means of the CVD technique. The HDS activity of Co–MoS_2/Al_2O_3 was increased by the calcination at 773 K but that of CVD-Co/Co–MoS_2/Al_2O_3 was unaltered and 95% of the activity of CVD-Co/MoS_2/Al_2O_3. Obviously, the calcination promotes the formation of a CoMoS phase, probably due to increased dispersion of Co caused by interactions between Co and Mo phases in the oxide state [4], whereas the effect of calcination on the extent of blocking by Co sulfide clusters is marginal (ca. 5%) at this catalyst composition. Since the formation of $CoAl_2O_4$ becomes extensive at a high calcination temperature [4], it is considered that an optimal calcination temperature is present for increasing the number of a CoMoS phase and for preventing the blocking, in particular at a high Co loading, where such blocking is important.

The amount of Co anchored in CVD-Co/Co–MoS_2/Al_2O_3 reflects the dispersion of MoS_2 particles in Co–MoS_2/Al_2O_3, as discussed above. The amount of anchored Co gradually decreases as the Co content increases above 4 wt% Co. This is ascribed to the blocking of the MoS_2 edges by Co sulfide clusters in Co–MoS_2/Al_2O_3. For instance, with 10 wt% Co–MoS_2/Al_2O_3, the incremental Co content (2.20 wt% Co) is 77% of that of MoS_2/Al_2O_3 (2.86 wt%) (Fig. 4), suggesting that 23% of the MoS_2 edges are blocked. In agreement with this, the HDS activity of CVD-Co/10 wt% Co–MoS_2/Al_2O_3 (248×10^{-5} mol/(g h)) is 79% of the activity of CVD-Co/MoS_2/Al_2O_3 (312×10^{-5} mol/(g h)) (Fig. 3).

4.4. Surface structure of Ni–MoS_2/Al_2O_3

As shown in Fig. 6, the activity of the CVD-Co/Ni–MoS_2/Al_2O_3 catalysts decreases slightly as the Ni content increases in the region below 1 wt% Ni, followed by a greater activity decrease above 1 wt% Ni. The amount of NO adsorption on Ni–MoS_2/Al_2O_3 increases linearly as the Ni content increases to 1 wt% Ni and shows a smaller increase above 1 wt% Ni. This catalytic and adsorption behavior is very similar to that observed for Co–MoS_2/Al_2O_3. Hence, it is rational to interpret the behavior in terms of the surface model proposed in Fig. 7 for Co–MoS_2/Al_2O_3.

If the Ni content is lower than 1 wt%, the edge sites of MoS_2 particles in Ni–MoS_2/Al_2O_3 are only partially occupied by Ni atoms forming a NiMoS phase and the vacant edge sites of MoS_2 particles become occupied by Co atoms to form a CoMoS phase, when Co is introduced by means of the CVD technique. It is proposed that both NiMoS and CoMoS phases are simultaneously present on the edges of the MoS_2 particles in the CVD-Co/Ni–MoS_2/Al_2O_3 catalysts. The slight decrease of the activity of CVD-Co/Ni–MoS_2/Al_2O_3 with increasing Ni content below 1 wt% is obviously due to the replacement of the CoMoS phase in CVD-Co/MoS_2/Al_2O_3 by a NiMoS phase with a slightly lower TOF of HDS under the present reaction conditions. It is considered that no catalytic synergies are observed between the coexisting CoMoS and NiMoS phases for the HDS of thiophene.

The activity of CVD-Co/Ni–MoS_2/Al_2O_3 significantly decreases as the Ni content increases above 1 wt% Ni. This fact can also be interpreted in terms of blocking of the active sites of Ni–MoS_2/Al_2O_3 by less active Ni sulfide clusters. The blocking starts above 1 wt% Ni for Ni–MoS_2/Al_2O_3 in contrast above 2 wt% Co for the Co counterpart. This might be due to a higher mobility and dispersion of Ni sulfide clusters than Co sulfide clusters (vide infra).

The important difference between Ni–MoS_2/Al_2O_3 and Co–MoS_2/Al_2O_3 is the activity change induced by Co incorporation by means of the CVD technique: an activity decrease in CVD-Co/Ni–MoS_2/Al_2O_3 above 2 wt% Ni in contrast to an increase in CVD-Co/Co–MoS_2/Al_2O_3. The activity increase in the latter catalyst is ascribed to an increase in the amount of CoMoS phase, as discussed above. The activity decrease in CVD-Co/Ni–MoS_2/Al_2O_3 is explained by assuming that the edge sites of MoS_2 particles are already filled by Ni atoms forming a NiMoS phase before the Co addition. As shown previously [33], the Co atoms anchored by the CVD technique slightly block the preexisting CoMoS phase by the formation of Co sulfide clusters, although most of the Co sulfide clusters form a harmless separate Co sulfide phase. Therefore, the slight decrease of the HDS activity of Ni–MoS_2/Al_2O_3 by the Co incorporation is ascribed to partial blocking of the NiMoS phase by the Co sulfide clusters.

It was reported that a redispersion of Ni sulfide clusters formed at a lower temperature takes place during sulfidation at a higher temperature, because of a lower thermal stability of the Ni sulfide clusters [22,24]. The redispersion of Ni sulfide clusters results in the effective formation of a NiMoS phase and even a NiWS phase to make Ni-WS_2/Al_2O_3 practical catalysts. It is considered that the higher coverage of Ni atoms on the edges of MoS_2 particles in Ni–MoS_2/Al_2O_3 results from the redispersion of Ni sulfide clusters during the sulfidation. The high thermal stability of Co sulfide clusters during sulfidation decreases the coverage of Co atoms on the edges of MoS_2 particles in Co–MoS_2/Al_2O_3 (Fig. 3) and renders the synergy in Co–WS_2/Al_2O_3 less effective. High mobility of Ni atoms on a MoS_2 basal plane was observed by means of STM [39]. The redispersion and high mobility of Ni atoms during sulfidation increases the coverage of

Ni atoms on the MoS_2 edges, whereas the blocking of the active sites in Ni–MoS_2/Al_2O_3 by Ni sulfide clusters starts at a lower content of the promoter (1 wt% Ni) than that in Co–MoS_2/Al_2O_3 (2 wt% Co).

The amount of Co anchored in Ni–MoS_2/Al_2O_3 is almost constant over a wide range of Ni content and identical with that anchored in Co–MoS_2/Al_2O_3. On the basis of these results, it is concluded that the amount of Co anchored by using $Co(CO)_3NO$ is a good measure of the dispersion of MoS_2 particles in Co(Ni)–Mo sulfide catalysts and that the dispersion of MoS_2 particles is not modified by the presence of Co or Ni and is independent of their amounts, in the case of the double-impregnation catalysts. It should be noted that this is limited to calcined Co(Ni)–Mo/Al_2O_3 catalysts with a Mo content higher than the monolayer loading [26].

5. Conclusions

In the present study, we evaluated the maximum potential activity of HDS catalysts to provide a guideline for development of ultradeep HDS catalysts. During the research, we found that it is also possible to characterize the surface structure of Al_2O_3-supported Co–Mo and Ni–Mo sulfide catalysts for HDS by using $Co(CO)_3NO$ as a probe molecule. The salient findings of the present study are as follows:

1. The Co *K*-edge XANES results confirmed that a selective formation of Co atoms constituting a CoMoS phase (model Co–Mo sulfide catalysts [26,27,33]) is achieved by means of the CVD technique using $Co(CO)_3NO$.
2. The HDS activity of CVD-Co/MoS_2/Al_2O_3 is the maximum potential activity of Co–MoS_2/Al_2O_3: the activity obtainable when the edges of MoS_2 particles are fully occupied by Co atoms without any blocking by Co sulfide clusters.
3. With Co–MoS_2/Al_2O_3, part of the edge sites of MoS_2 particles remain unoccupied by Co atoms in a wide range of Co content. In contrast, with the Ni counterpart, the edges of MoS_2 particles are completely occupied by Ni atoms above 2 wt% Ni.
4. Blocking of the active sites by overlayers of Co(Ni) sulfide clusters decreases the HDS activity to a considerable extent.
5. The CVD technique using $Co(CO)_3NO$ as a probe molecule provides a novel characterization method of Co(Ni)–Mo sulfide catalysts. One can obtain information on (i) the maximum potential HDS activity, (ii) the extent of blocking of the active phase, (iii) the coverage of Co(Ni) atoms on the edges of MoS_2 particles, and (iv) the dispersion of the MoS_2 particles in Co(Ni)–MoS_2 catalysts.

Acknowledgment

This work has been entrusted by the New Energy and Industrial Technology Development Organization under a subsidy of the Ministry of Economy, Trade, and Industry.

References

[1] C. Song, Am. Chem. Soc. Div. Fuel Chem. Prepr. 47 (2002) 438.
[2] K.G. Knudsen, B.H. Cooper, H. Topsøe, Appl. Catal. A 189 (1999) 205.
[3] R. Prins, in: G. Ertl, H. Knözinger, H.J. Weitkamp (Eds.), Handbook of Heterogeneous Catalysis, VCH, Weinheim, 1997, p. 1908.
[4] H. Topsøe, B.S. Clausen, F.E. Massoth, in: J.R. Anderson, M. Boudard (Eds.), Catalysis Science and Technology, vol. 11, Springer, Berlin, 1996.
[5] T. Kabe, A. Ishihara, W. Qian, Hydrodesulfurization and Hydrodenitrogenation, Kodansha, Tokyo, 1999.
[6] D.D. Whitehurst, T. Isoda, I. Mochida, Adv. Catal. 42 (1998) 345.
[7] J.A.R. van Veen, E. Gerkema, A.M. van der Kraan, A. Knoester, J. Chem. Soc., Chem. Commun. (1987) 1684.
[8] J.A.R. van Veen, E. Gerkema, A.M. van der Kraan, P.A.J.M. Hendriks, H. Beens, J. Catal. 133 (1992) 112.
[9] T. Shimizu, K. Hiroshima, T. Honma, T. Mochizuki, M. Yamada, Catal. Today 45 (1998) 271.
[10] S.P.A. Louwers, R. Prins, J. Catal. 133 (1992) 94.
[11] L. Medici, R. Prins, J. Catal. 163 (1996) 38.
[12] R. Iwamoto, J. Grimblot, Adv. Catal. 44 (2000) 417.
[13] M. Sun, D. Nicosia, R. Prins, Catal. Today 86 (2003) 173.
[14] O. Poulet, R. Hubaut, S. Kasztelan, J. Grimblot, Bull. Soc. Chim. Belg. 108 (1991) 857.
[15] J. Ramirez, V.M. Castano, C. Leclercq, A. Lopez Agudo, Appl. Catal. A 83 (1992) 252.
[16] J.A.R. van Veen, H.A. Colijn, P.A.J.M. Hendriks, A.J. Welsenes, Fuel Proc. Technol. 35 (1993) 137.
[17] B.S. Clausen, S. Mørup, H. Topsøe, R. Candia, J. Phys. Colloq. C 6 (1976) 37.
[18] N.Y. Topsøe, H. Topsøe, J. Catal. 75 (1982) 354.
[19] H. Topsøe, B.S. Clausen, N.Y. Topsøe, E. Pederson, Ind. Eng. Chem. Fundam. 25 (1986) 25.
[20] R. Candia, O. Sørensen, J. Villadsen, N.Y. Topsøe, B.S. Clausen, H. Topsøe, Bull. Soc. Chim. Belg. 93 (1984) 763.
[21] A.M. de Jong, V.H.J. de Beer, J.A.R. van Veen, J.W. Niemantsverdriet, J. Phys. Chem. 100 (1996) 17722.
[22] G. Kishan, L. Coulier, J.A.R. van Veen, J.W. Niemantsverdriet, J. Catal. 196 (2000) 180.
[23] G. Kishan, L. Coulier, J.A.R. van Veen, J.W. Niemantsverdriet, J. Catal. 200 (2001) 194.
[24] L. Coulier, G. Kishan, J.A.R. van Veen, J.W. Niemantsverdriet, J. Phys. Chem. 106 (2002) 5897.
[25] T. Kubota, N. Hosomi, K. Bando, T. Matsui, Y. Okamoto, Phys. Chem. Chem. Phys. 5 (2003) 4510.
[26] Y. Okamoto, S. Ishihara, M. Kawano, M. Satoh, T. Kubota, J. Catal. 217 (2003) 12.
[27] Y. Okamoto, K. Ochiai, M. Kawano, K. Kobayashi, T. Kubota, Appl. Catal. A 226 (2002) 115.
[28] Y. Okamoto, M. Kawano, T. Kubota, J. Chem. Soc., Chem. Commun. (2003) 1086.
[29] C. Wivel, R. Candia, B.S. Clausen, S. Morup, H. Topsøe, J. Catal. 68 (1981) 453.
[30] S.M.A.M. Bouwens, J.A.R. van Veen, D.C. Koningsberger, V.H.J. de Beer, R. Prins, J. Phys. Chem. 95 (1991) 123.
[31] M.W.J. Crajé, S.P.A. Louwers, V.H.J. de Beer, R. Prins, A.M. van der Kraan, J. Phys. Chem. 96 (1992) 5445.

[32] W. Niemann, B.S. Clausen, H. Topsøe, Catal. Lett. 4 (1990) 355.
[33] Y. Okamoto, T. Kubota, Catal. Today 86 (2003) 31.
[34] F. Maugé, A. Vallet, J. Bachelier, J.C. Duchet, J.C. Lavalley, J. Catal. 162 (1996) 88.
[35] M.W.J. Crajé, V.H.J. de Beer, A.M. van der Kraan, Appl. Catal. 70 (1991) L7.
[36] M.W.J. Crajé, V.H.J. de Beer, A.M. van der Kraan, Bull. Soc. Chim. Belg. 100 (1991) 953.
[37] A.M. van der Kraan, M.W.J. Crajé, E. Gerkema, W.L.T.M. Ramselaar, V.H.J. de Beer, Hyperfine Interact. 46 (1989) 567.
[38] Y. Okamoto, T. Kawabata, T. Kubota, I. Hiromitsu, Chem. Lett. (2003) 1150.
[39] J.G. Kushmerick, P.S. Weiss, J. Phys. Chem. B 102 (1998) 10094.